Completely Digital Position Feedback Control for Synchronous Servodrives

DIETRICH NAUNIN, DIETER HETZEL, HANS-CHRISTIAN REUSS, AND CHRISTIAN ERIC SECHELMANN

***Abstract*—A completely digital control concept for a synchronous servodrive is presented. The hardware consists of a pulsewidth modulated (PWM) inverter and a microcontroller with peripheral components for state value measurements and set value output. The derivation of a mathematical model of the PM synchronous servodrive is shown. A new cascaded state feedback controller, which consists of a position state feedback controller with an inner current control loop, is introduced. Two different types of current controllers are compared.**

I. Introduction

The requirements of automation applications are continuously rising. Higher dynamic ac motors, faster and higher integrated microcomputers, and faster switching power semiconductors enable the development of more effective systems. Therefore a new control structure has been chosen to fit the requirements of high dynamic positioning.

State of the art of servodrive control systems is a traditional structure containing a digital position feedback control loop with inner analog speed and current control loops. Disadvantages of this concept are drift and noise problems of the analog circuits and interfaces, inflexibility of the chosen controller parameters and the need of separate speed and position sensors.

The new system is realized only by digital means, no analog control circuits are used any more [1]. Furthermore the concept allows the realization of a multi-axis control system (e.g., for robot control) with decentralized intelligence.

Fig. 1 shows the structure of a control system with intelligent axis controllers. They are supplied with position information by a master computer.

Each axis consists of the following:

- a synchronous machine with a three phase stator winding and a $SmCo_5$-PM disc rotor;
- a pulse controlled inverter with six power MOSFET's and;
- a 16 bit single-chip-microcomputer with I/O modules.

The single chip microcomputer measures the state values (torque, speed, and position) of the dedicated machine and calculates the set values by an implemented control algorithm in order to reach the reference position given by the master computer.

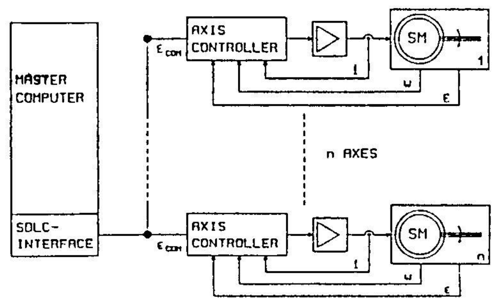

Fig. 1. Robot control system.

The most interesting points of this paper are design, simulation and practical implementation of completely digital position feedback control structures in an inexpensive microcomputer system.

Considering well-known control structures as cascade control and state feedback control a new controller has been developed: a current control loop with a superposed position state feedback controller.

II. Hardware

It was an aim to bring the axis controller into a very compact form. Therefore the microcontroller 8096 (INTEL) was chosen because it contains various integrated on chip peripheral devices like serial and parallel ports, programmable high speed input/output pins, an analog to digital converter and a PWM output. In addition to these functional units there are a clock generator, timers and an interrupt logic. The average instruction execution time is about 1 to 2 μs.

Since the microcomputer has a von-Neumann-structure three tasks must be executed at the same time using a special interrupt structure (Fig. 2).: initialization (level 1) and communication (level 4) take place in the main program. Commutation and feedback control is done in the interrupt driven levels 2 and 3.

The sampling time of the control algorithm is 1.024 ms. Every 256 μs the voltage space-phasor is readjusted according to the actual rotor position.

Measurement of the State Values

Several hardware modules have been realized for the measurement of the state values (Fig. 3). These plug-in

Manuscript received April 12, 1989; revised February 23, 1990. This paper was presented at the 1989 IEEE Power Electronics Specialists Conference, Milwaukee, WI, June 26-29.
The authors are with Technische Universitat Berlin, Institut fur Elektronik, Einsteinufer 17, D-1000 Berlin 10, F.R. Germany.
IEEE Log Number 9037437.

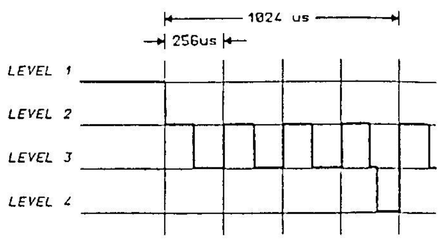

Fig. 2. Software priority levels. Level 1: initialization. Level 2: commutation. Level 3: control. Level 4: communication.

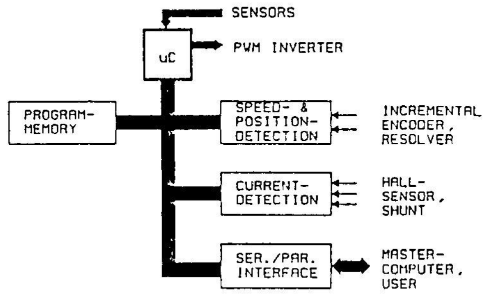

Fig. 3. Structure of microcontroller.

modules allow a maximum of flexibility for different state value sensor interfaces. Only one small module has to be changed to connect a new sensor.

The control system does not require a tachogenerator. The position of the axis is detected by a high resolution position sensor and the motor speed is calculated from the position values via a derivation by time.

Position sensor interfaces for incremental encoders and resolvers are available. For the resolution and accuracy 13 bit are guaranteed for the incremental encoder and better than 10 bit for the resolver up to a maximum speed of 5000 r/min.

Also two different types of modules are available for current measurements. Both measure the average currents in all three stator windings over a PWM period to eliminate the ripple influence. The current values are converted to voltage signals by Hall sensors or shunts.

The low-cost module consists of voltage controlled oscillators that convert the Hall sensor output signals into frequencies. These frequencies are proportional to the current values and are counted over a PWM period.

The second type of module determines the values of the average currents by the aid of analog integrators and succeeding 12 bit A/D converters.

Communication with the Master

The communication takes place via a high speed serial interface with a SDLC protocol. This interface is also realized as a plug-in module and therefore an adaption to other communication protocols is quite simple.

MOSFET PWM Inverter

The power inverter is realized with six MOSFET's (Siemens BSM 151, 500 V, 56 A). They form three half-bridges that are connected to the three windings of the star-connected machine. The connection to the controller is implemented by optocouplers, a programmable logic, and special driver circuits (Fig. 4).

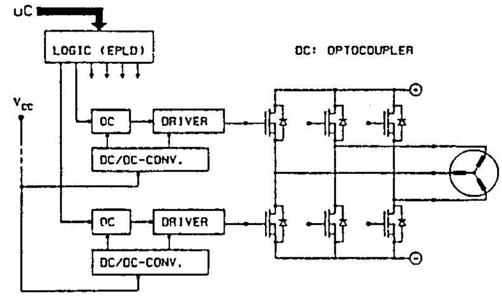

Fig. 4. The MOSFET PWM inverter.

III. Mathematical Model of the Synchronous Servodrive

The synchronous servodrive used in the presented project has three-phase stator windings and an eight-pole disc rotor with $SmCo_5$-magnets. Some technical data are given next [2]:

power (continuous duty)	P	1150 W
torque (3000 r/min)	M	3.6 Nm
peak torque	M_j	35 Nm
maximum speed	n	6000 r/min
mechanical time constant	T_m	3.9 ms
electrical time constant	T_{el}	2.8 ms.

In order to find a mathematical description of the $SmCo_5$-PM synchronous machine, the following simplifying assumptions can be made [7, p. 143], [8]:

- the PM excited field can not be weakened ($|\vec{\psi}_p| =$ const),
- the armature inductance is independent of the rotor position (no salient pole rotor).

The instantaneous values of the phase currents and voltages of the star-connected machine are combined to space-phasors in the stator reference system as shown in (1) and (2) [3, p. 34]. The indices S (stator) and R (rotor) denote the reference systems:

$$\vec{i}_s = \frac{2}{3}\,[1 \;\; \alpha \;\; \alpha^2] \begin{bmatrix} i_A \\ i_B \\ i_C \end{bmatrix} \tag{1}$$

$$\vec{u}_s = \frac{2}{3}\,[1 \;\; \alpha \;\; \alpha^2] \begin{bmatrix} u_A \\ u_B \\ u_C \end{bmatrix} \tag{2}$$

with

$$\alpha = e^{j(2/3)\Pi}. \tag{3}$$

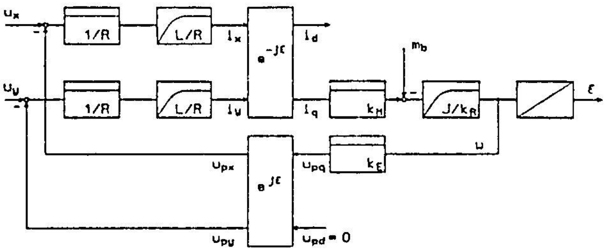

Fig. 5. Block diagram of SM in stator reference system.

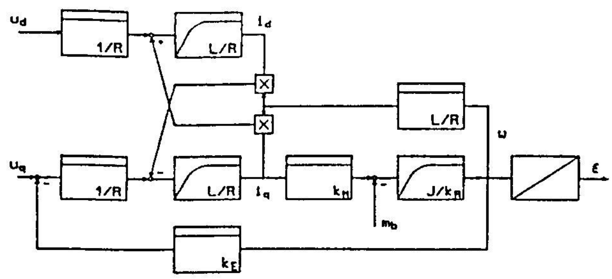

Fig. 6. Model of the SM in rotor reference system.

The variable ϵ denotes the electrical rotor position; the angular rotational speed is defined by

$$\omega = \frac{d\epsilon}{dt}. \tag{4}$$

The EMF space-phasor of the machine is given by

$$\vec{u}_p = j\omega \cdot \vec{\psi}_p = j\omega \cdot k_E e^{j\epsilon} \tag{5}$$

with

$$k_E = |\vec{\psi}_p|. \tag{6}$$

The voltage equation describing the dynamic behavior of the PM excited synchronous machine in the stator reference system has the following form [7, p. 263], [8, p. 83]:

$$\vec{u}_S = L\frac{d}{dt}\vec{i}_S + R\vec{i}_S + \vec{u}_p. \tag{7}$$

The mechanical behavior of the servodrive can be described by

$$J\frac{d\omega}{dt} = k_M \cdot \mathrm{Im}\left\{\vec{i}_S \cdot e^{-j\epsilon}\right\} - m_b - k_r \cdot \omega \tag{8}$$

with

$$k_M = \tfrac{3}{2} p k_E. \tag{9}$$

In (8) m_b represents the load torque and $k_r \cdot \omega$ the frictional torque, while p denotes the number of pole pairs.

In Fig. 5 the block diagram of the machine is shown according to (7) and (8) with the indices x and y of the space-phasor in the stator reference system.

In many applications it was found more convenient to transform the voltage equation (7) into the rotor reference system. The space-phasors in the rotor reference system are given by [3, p. 263]:

$$\vec{u}_R = u_d + ju_q = \vec{u}_S e^{-j\epsilon} \tag{10}$$

$$\vec{i}_R = i_d + ji_q = \vec{i}_S e^{-j\epsilon}. \tag{11}$$

The voltage equation of the PM excited synchronous motor in the rotor reference system can be determined from (7) by using (10) and (11) [8, p. 83]:

$$\vec{u}_R = L \cdot \frac{d\vec{i}_R}{dt} + R \cdot \vec{i}_R + j\omega L \cdot \vec{i}_R + j\omega k_E. \tag{12}$$

The transformation of the current term in (8) describing the electrical torque component results in

$$J\frac{d\omega}{dt} = k_M \cdot i_q - m_b - k_r \cdot \omega. \tag{13}$$

Fig. 6 shows the block diagram of the machine in the rotor reference system using (12) and (13).

IV. Control Structures

A feedback control circuit is set up that is fully digital and performed by means of a microcomputer. This has the advantage, that the control structure can be easily changed by programming a new software algorithm. The input values of the digital controller are the command variable ϵ_{com} and the state variables ϵ, ω and $\vec{i}$. The output value of the digital controller is the voltage space-phasor $\vec{u}_S$ (7).

A well-known and widely used controller for electrical servodrives is the cascade controller [7]. It consists of a position feedback controller with inner speed and current control loops. The current loop forming the innermost control function may be regarded as an impressed current source. Since the sequence torque-speed-position conforms very well to the structure of the plant, the cascade controller has the following advantages [7]:

- design and commissioning can be achieved step by step regarding only one part of the system at one time beginning with the current loop, and;
- by limiting internal variables (e.g., i_q) protective functions can be easily implemented.

The advantage of the simple design and commissioning can be only used under the assumption, that the bandwidth of the control increases towards the inner loops with the current loop being the fastest and the position loop being the slowest.

To meet especially the requirements of the inner loop only by digital means, i.e., suitable sampling times, a very expensive hardware has to be set up. It can be shown, that a cascade controller structure using the same sampling rate for all control loops can be converted into a state feedback controller structure, while the opposite does not hold. Thus the state feedback controller allows more freedom in controller design. It has the advantage that a defined dynamical behavior of the entire system can be performed. However inner variables can not be limited and the commissioning of the state feedback controller is more difficult due to the complex determination of the control factors.

In the presented project a structure was developed that combines the principles of cascade control and state feedback control. This digital cascaded state feedback controller consists of two subsystems: an inner current loop and a superposed position state feedback controller (Fig. 7). Because of the calculation time of the microcomputer the digital control systems contains a dead time block. In this application the dead time is equal to the sampling time $T = 1$ ms. In Fig. 8 a timing diagram of the feedback control is shown. At the time $(n - 1) \cdot T$ the actual state values are measured and the command position ϵ_{com} is passed to the controller. At the time $n \cdot T$ the output of the calculated voltage space-phasor becomes valid.

Current Feedback Control

Current feedback control can be realized either in the rotor or in the stator reference system. Both control structures will be introduced and compared.

Rotor Reference System: The model described in Section III and shown in Fig. 6 is nonlinear because of the coupling terms $i_d \cdot \omega$ and $i_q \cdot \omega$, which couple the direct and the quadrature axis. In order to get a linear model the following voltage space-phasors are defined [4]:

$$\vec{u}_{R,\text{disturb}} = j\omega L \cdot \vec{i}_R + j\omega k_E \tag{14}$$

$$\vec{u}_{R,\text{lin}} = \vec{u}_R - \vec{u}_{R,\text{disturb}} \tag{15}$$

Equation (12) describing the model of the synchronous machine can now be written in the following form:

$$\vec{u}_{R,\text{lin}} = L \cdot \frac{d\vec{i}_R}{dt} + R \cdot \vec{i}_R. \tag{16}$$

Equations (16) and (13) lead to the block diagram shown in Fig. 9. The current i_d does not influence the electric torque. Splitting up (16) into the real and imaginary components d and q and leaving out the indices leads to the same expression for each component:

$$\frac{di}{dt} = \frac{1}{L} \cdot u_{\text{lin}} - \frac{R}{L} \cdot i. \tag{17}$$

For this differential equation a time-discrete solution can be found:

$$i_{n+1} = Ai_n + \frac{(1 - A)}{R} u_{\text{lin},n} \tag{18}$$

with

$$A = e^{-(R/L)T}. \tag{19}$$

Using the z-transform the transfer function of the electrical part of the plant can be calculated:

$$T_E(z) = \frac{i(z)}{u_{\text{lin}}(z)} = \frac{1 - A}{R(z - A)}. \tag{20}$$

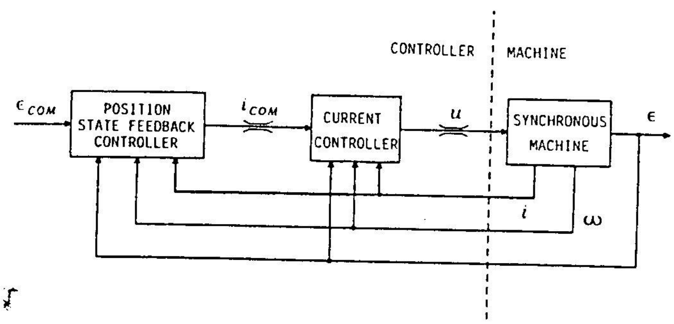

Fig. 7. Realized control structure.

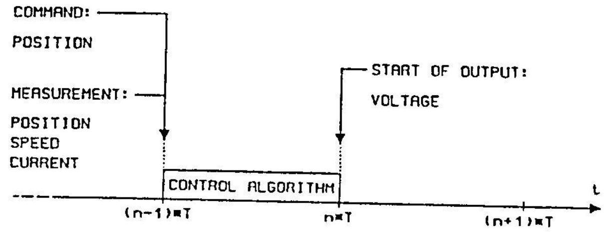

Fig. 8. Timing diagram of feedback control.

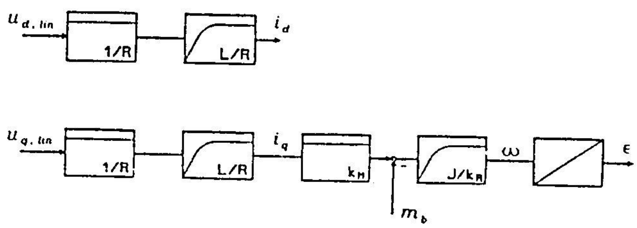

Fig. 9. Linearized model of SM in rotor reference system.

The control law for a dead-beat current feedback controller can be found by using (18) twice to calculate i_{n+1} from i_{n-1}:

$$\vec{u}_{R\text{lin},n} = B \cdot \vec{i}_{R\text{com},n-1} - BA^2 \cdot \vec{i}_{R,n-1} - A \cdot \vec{u}_{R\text{lin},n-1} \tag{21}$$

with

$$B = \frac{R}{(1 - A)}. \tag{22}$$

It is obvious, that the current control laws for the current components are identical. Using this controller the following calculations have to be done. The voltage $\vec{u}_{\text{disturb}}$ is introduced in order to compensate the voltage $\vec{u}_{\text{comp}}$ (Fig. 10):

$$\vec{i}_{R,n-1} = \vec{i}_{S,n-1} \cdot e^{-j\epsilon_{n-1}} \tag{23}$$

$$\vec{u}_{R\text{comp},n} = j\omega_{n-1} \cdot (L \cdot \vec{i}_{R,n-1} + k_E) \tag{24}$$

$$\vec{u}_{R,n} = \vec{u}_{R\text{lin},n} + \vec{u}_{R\text{comp},n} \tag{25}$$

$$\vec{u}_{S,n} = \vec{u}_{R,n} \cdot e^{j \cdot (\epsilon_{n-1} + \omega_{n-1} \cdot T)}. \tag{26}$$

In (26) the calculation time of the control algorithm is taken into account. According to the dead-beat character-

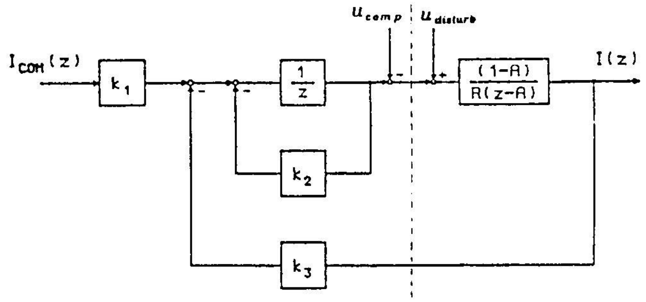

Fig. 10. Feedback control structure of one current component.

istic of the current feedback controller the command transfer function for each closed current feedback control loop results in

$$T_{curr}(z) = \frac{1}{z^2}. \tag{27}$$

Stator Reference System

With the voltage space-phasors

$$\vec{u}_{S\text{disturb}} = j\omega k_E \cdot e^{j\epsilon} \tag{28}$$

$$\vec{u}_{S,\text{lin}} = \vec{u}_S - \vec{u}_{S,\text{disturb}}. \tag{29}$$

Equation (7) takes the form

$$\vec{u}_{S,\text{lin}} = L \cdot \frac{d\vec{i}_S}{dt} + R \cdot \vec{i}_S. \tag{30}$$

The comparison of (16) and (30) shows, that the control law for the dead-beat current feedback controller in the stator reference system is identical with (21):

$$\vec{u}_{S\text{lin},n} = B \cdot \vec{i}_{S\text{com},n-1} - BA^2 \cdot \vec{i}_{S,n-1} - A \cdot \vec{u}_{S\text{lin},n-1}. \tag{31}$$

With this controller the following calculations have to be done:

$$\vec{i}_{S\text{com},n-1} = \vec{i}_{R\text{com},n-1} \cdot e^{j\cdot(\epsilon_{n-1} + 1.5\cdot\omega_{n-1}\cdot T)} \tag{32}$$

$$\vec{u}_{S\text{comp},n} = jk_E\omega_{n-1} \cdot e^{j\cdot(\epsilon_{n-1} + 1.5\cdot\omega_{n-1}\cdot T)} \tag{33}$$

$$\vec{u}_{S,n} = \vec{u}_{S\text{lin},n} + \vec{u}_{S\text{comp},n}. \tag{34}$$

Fig. 10 shows the block diagram of the current feedback controller for one current component. The block diagram is valid for the controllers in the rotor and the stator reference system.

Fig. 11 shows the structure of the current feedback control in the stator reference system. Each of the two current feedback control loops has the structure shown in Fig. 10.

Comparison of the Current Feedback Controllers

A digital simulation of the two current feedback controllers with a given square wave command function $i_{q\text{com}}$ was carried out. The starting value of the angular rotor speed used in the simulation was $\omega_0 = 754\ \text{s}^{-1}$ (el). The variation of the angular rotor speed ω in the shown period of time is neglectable. The results of the simulation are shown in Fig. 12 (controller in the rotor reference system) and Fig. 13 (controller in the stator reference system).

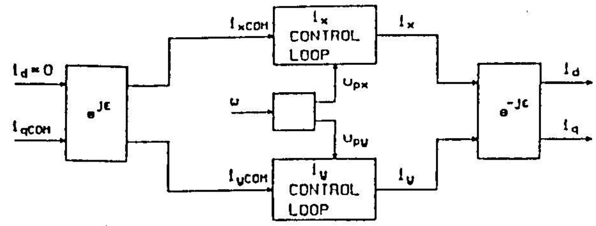

Fig. 11. Current feedback control in stator reference system.

It is evident, that the stator-oriented controller provides better results while the calculation time for both algorithms is almost the same. The better dynamic behaviour of the stator oriented feedback controller results from the fact, that the obsolete phasor $\vec{i}_{R,n-1}$ has to be used instead of the correct but unknown phasor $\vec{i}_{R,n}$ in (24). An improvement of the performance of the rotor-oriented feedback controller can be achieved—on cost of the calculation time—by using (18) for the calculation of the unknown phasor $\vec{i}_{R,n}$.

Position State Feedback Control

Equation (13) describing the speed behavior of the servodrive can be written in the following form (the unknown load torque m_b is neglected):

$$\frac{d\omega}{dt} = \frac{k_M}{J} \cdot i_q - \frac{k_r}{J} \cdot \omega. \tag{35}$$

The current i_q is calculated as the mean value of the current values $i_{q,n}$ and $i_{q,n+1}$:

$$i_q = \frac{i_{q,n} + i_{q,n+1}}{2}. \tag{36}$$

The time-discrete description of the rotor speed can now be obtained by solving (35):

$$\omega_{n+1} = B\omega_n + (1 - B)\frac{k_M}{k_r} \cdot \frac{i_{q,n} + i_{q,n+1}}{2} \tag{37}$$

with

$$B = e^{-(k_r/J)\cdot T}. \tag{38}$$

The ω-transfer function in the z-plane is given by

$$\omega(z) = \frac{k_M(1 - B)(z + 1)}{2k_r(z - B)} \cdot i_q(z). \tag{39}$$

The rotor position can be calculated by the integration of the rotor speed:

$$\epsilon(\tau) = \epsilon_0 + \int_0^{\tau} \omega(t)\, dt. \tag{40}$$

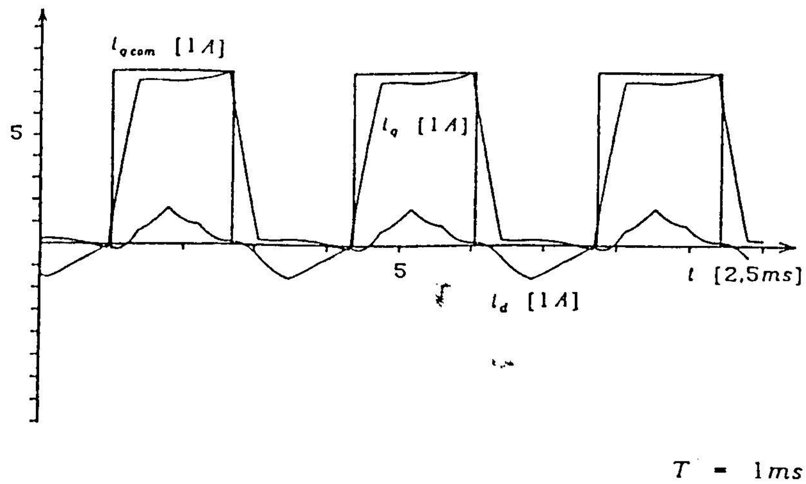

Fig. 12. Step responses of current feedback controller in rotor reference system.

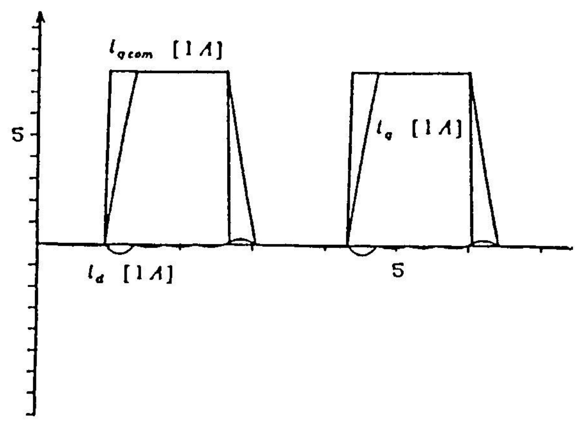

Fig. 13. Step responses of current feedback controller in stator reference system.

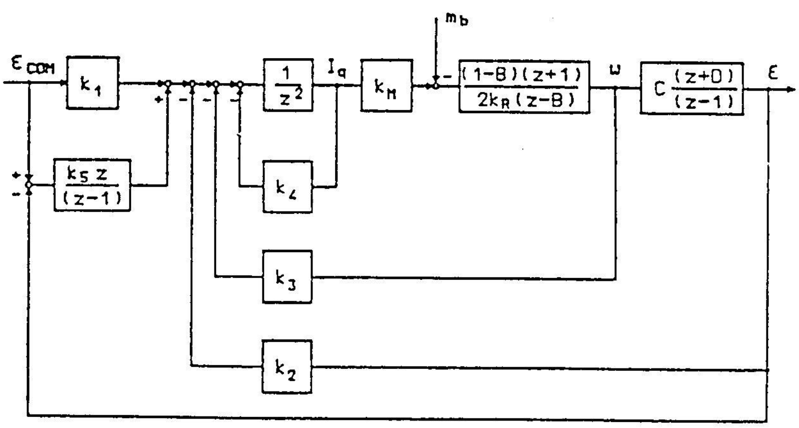

Fig. 14. Position state feedback controller.

Using this equation a time-discrete description of the position behavior can be obtained:

$$\epsilon_{n+1} = \epsilon_n + \frac{J}{k_r}(1 - B) \cdot \omega_n + \left(T + \frac{J}{k_r}(B - 1)\right) \frac{k_M}{k_r} \cdot \frac{i_{q,n} + i_{q,n+1}}{2}. \quad (41)$$

Herefrom the ϵ-transfer function can be derived:

$$\epsilon(z) = C \cdot \frac{z + D}{z - 1} \cdot \omega(z). \quad (42)$$

Designing a position state feedback controller an integrator for the position should be implemented in order to avoid steady state errors caused by the load torque. This

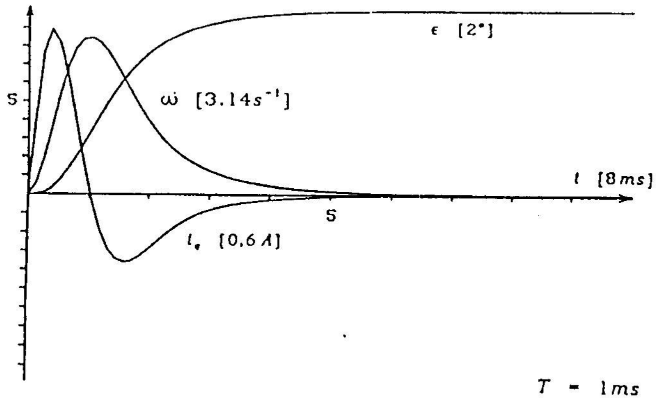

Fig. 15. Command step response of position state feedback controller (simulation).

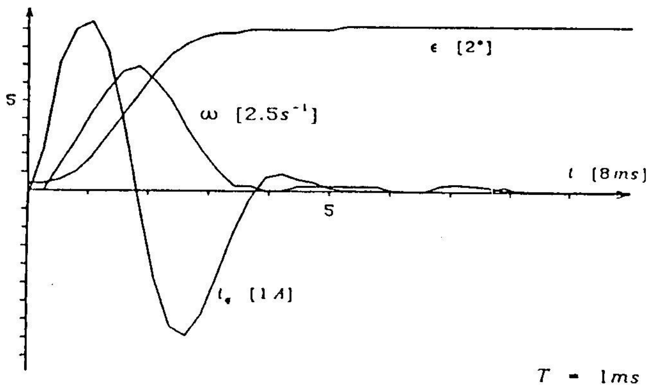

Fig. 16. Command step response of position state feedback controller (measurement).

is the reason why the control law in the z-plane has the following form:

$$I_{q\text{com}} = k_1 \epsilon_{\text{com}} - k_2 \epsilon - k_3 \omega - k_4 I_q + k_5 \cdot \frac{z}{z-1} (\epsilon_{\text{com}} - \epsilon). \quad (43)$$

Fig. 14 shows the structure of the position state feedback controller according to (43). The transfer function of the closed current control loop is used according to (27). The command transfer function of the introduced position control loop assumes the following form:

$$T_p(z) = \frac{\epsilon(z)}{\epsilon_{\text{com}}(z)} = E \cdot \frac{z^3 + \alpha_2 z^2 + \alpha_1 z^1 + \alpha_0}{z^5 + \beta_4 z^4 + \beta_3 z^3 + \beta_2 z^2 + \beta_1 z^1 + \beta_0}. \quad (44)$$

The zeroes of the denominator polynomial are determined by the pole assignment method. Here from the gain factors $k_1 \ldots k_5$ can be derived. The calculations during the controller design and the simulations of the closed control loops using the Runge–Kutta-method are executed by a personal computer. Figs. 15 and 16 show the simulated and the measured responses on a command position step of $\epsilon_{\text{com}} = 20°$. Small variations of the curve shapes are caused by different inertia torques in the simulation and the real system.

V. Conclusion

The results achieved up to now show that the step from analog/digital control circuits for synchronous servodrives to completely digital ones can be done applying inexpensive 16-bit single chip microcomputers and MOSFET pulse controlled inverters. For the implementation as software algorithm a cascaded state feedback controller, which combines the advantages of the cascade and the state feedback control structure, has been introduced. This controller consists of a current control loop with a superposed position state feedback controller. It has been proven that a realization of the current control loop in the stator reference system should be preferred. The entire position control system shows a good dynamic behavior.

References

[1] D. Naunin and H. C. Reuss, "Synchronous servodrive: A very compact solution of control problems by means of a single-chip-microcomputer," in *Proc. IEEE IAS Annual Meeting*, Pittsburgh, PA, 1988.

[2] N. N., Drehstrom-Hochleistungs-Servomotoren, Serie SE, INFRANOR GmbH, Heidelberg, 1985.

[3] H. Bühler, Einführung in die Theorie geregelter Drehstromantriebe Band 1, Basel: Birkhäuser Verlag, 1971.

[4] D. Hetzel, Digitale Regelung eines Permanentmagnet-Synchronantriebes, Diplomarbeit, TU-Berlin, 1989.

[5] D. Naunin, M. Kindscher, C. Sechelmann, and H. C. Reuss, "Mikrorechnergesteuerter Synchronservomotor mit Lagezustandsregelung," ETG-Fachbericht 27, 1989, pp. 81–90.

[6] D. Naunin, K. Cevik, and H. C. Reuss, "New Concepts for Controlling Servodrives in Robots," in *Proc. IEEE Int. Workshop on Robotics*, Madrid, Spain, 1987.

[7] W. Leonhard, *Control of Electrical Drives*. Springer-Verlag: Berlin, Heidelberg, New York, Tokyo, 1985.

[8] B. Orlik, "Regelung einer permanentmagneterregten Synchronmaschine mit einem Mikrorechner," Automatisierungstechnik, vol. 33, no. 3, 1985, pp. 82–88.

Dietrich Naunin was born in Münster, West Germany in 1937. He received the Dipl.-Ing. degree from the University of Aachen, Aachen, West Germany, and the Ph.D. degree from the Technical University of Berlin, Berlin, West Germany, in 1963 and 1968, respectively.

Since 1972, he has been Professor of Electrical Engineering at the Technical University of Berlin. In 1973–1974 he spent several months as a Visiting Professor at the Massachusetts Institute of Technology, Cambridge, MA.

His research interests are primarily in the area of electric drives, especially their control by microcomputers, in robotics and electric cars. He is author of several books and currently President of the German Electric Vehicle Society.

Dieter Hetzel received the Dipl.-Math. (M.Sc.) degree in mathematics from the Technical University of Berlin, Berlin, West Germany, in 1976.

After several years of industrial employment he began his studies at the Institute of Electronics of the Technical University of Berlin and is scheduled to receive the Dipl.-Ing. degree in 1990.

Hans-Christian Reuss was born in Düsseldorf, West-Germany, on February 6, 1959. He received the Dipl.Ing. (M.S.) and the Ph.D. degrees in electrical engineering from the Technical University of Berlin, Berlin, West Germany, in 1984 and 1989, respectively.

From 1984 to 1989 he was with the Institute of Electronics, Technical University of Berlin, as an Assistant (teaching and R&D) to Prof. Naunin, where he was engaged in the development of completely digital control systems for high dynamic servodrives.

In 1989 Dr. Reuss joined the PHILIPS Components Application Laboratory in Hamburg, West-Germany, where he is presently involved in the development of serial in-vehicle networks, and design of microcontrollers for automotive applications.

Christian Eric Sechelmann was born in Berlin, West Germany on December 2, 1960. He received the Dipl.-Ing. degree in electrical engineering from the Technical University of Berlin, Berlin, West Germany, in 1987.

In April 1987 he joined the Institute of Electronics of the Technical University of Berlin, where he is currently working as a scientific assistant.

His research interests include adaptive control of synchronous servodrives in robotic applications.